Biocatalysis

International Edition: DOI: 10.1002/anie.201412049
German Edition: DOI: 10.1002/ange.201412049

Individual Surface-Engineered Microorganisms as Robust Pickering Interfacial Biocatalysts for Resistance-Minimized Phase-Transfer Bioconversion**

Zhaowei Chen, Haiwei Ji, Chuanqi Zhao, Enguo Ju, Jinsong Ren, and Xiaogang Qu**

Abstract: *A powerful strategy for long-term and diffusional-resistance-minimized whole-cell biocatalysis in biphasic systems is reported where individually encapsulated bacteria are employed as robust and recyclable Pickering interfacial biocatalysts. By individually immobilizing bacterial cells and optimizing the hydrophobic/hydrophilic balance of the encapsulating magnetic mineral shells, the encased bacteria became interfacially active and locate at the Pickering emulsion interfaces, leading to dramatically enhanced bioconversion performances by minimizing internal and external diffusional resistances. Moreover, in situ product separation and biocatalyst recovery was readily achieved using a remote magnetic field. Importantly, the mineral shell effectively protected the entire cell from long-term organic-solvent stress, as shown by the reusability of the biocatalysts for up to 30 cycles, while retaining high stereoselective catalytic activities, cell viabilities, and proliferative abilities.*

Whole-cell biocatalysis in aqueous/organic biphasic systems is an elegant method to transform poorly water-soluble substrates into fine chemicals, pharmaceuticals, and fuels.[1] However, long-term exposure to organic solvents and especially to vigorous mixing to facilitate mass transfer between two phases can easily lead to fatal cell destruction.[1d] Consequently, immobilization of microbes in supports, such as silica matrices or alginate beads, has been used to improve microbial performance and stability. Nevertheless, the accessibility of biocatalysts by substrates in these systems suffers from two intractable diffusional limitations.[1a] The first limitation, namely the external diffusional limitation, stems from the limited organic–aqueous interfaces across which mass transfer should take place. The second issue is an internal diffusional limitation which is as a result of the fact that these systems generally deal with the entrapment of a collection of cells and thus substrates have to diffuse inside the supports. As a result, the catalytic efficiency of these immobilized biocatalysts is undesirably diminished. Thus, the design of an ideal immobilization technique for overcoming both diffusional limitations and at the same time providing long-term stability has remained a great challenge in this field.

As a rapidly emerging class of biphasic reaction, Pickering interfacial catalysis, where colloid particles can simultaneously stabilize an emulsion and catalyze reactions at the interface of two immiscible solvents, has become an attractive research topic.[2] In such systems the location of particles at Pickering interfaces not only maximizes the extent of the liquid–catalyst–liquid interfacial areas and facilitates mass transfer between the two phases but also relieves transport limitations. Such improvements could have a major impact in the field of whole-cell biphasic biocatalysis. Although it seems promising to assemble biocatalytically active bacteria as "soft" particles[3] at the liquid–liquid interface for biphasic reactions because of the vulnerability of bacteria towards organic solvents and the lack of interfacial activity to stabilize emulsions,[4] the application of bacteria as Pickering interfacial biocatalysts is uncommon and is difficult to perform. Recently, a chitosan–bacteria complex was shown to be able to place bacteria at Pickering interfaces[4] although the antimicrobial activity of chitosan and the difficulties in bacteria recovery would hamper further interfacial biocatalytic studies. Accordingly, we envision that exploring properly surface-engineered bacteria as robust Pickering interfacial biocatalysts would provide the possibility to address all the above mentioned challenges.

We herein describe a simple yet powerful new strategy for long-term and diffusional-resistance-minimized whole-cell biocatalysis in biphasic systems by utilizing individually encapsulated microbes as robust and recyclable Pickering interfacial biocatalysts. Encapsulation of individual living cells within robust artificial shells promises great potential to functionalize cell surfaces at the single-cell level and protect cells against harsh conditions.[5] As shown in Scheme 1, individual *Alcaligenes faecalis* ATCC 8750 cells were firstly coated with a porous calcium phosphate (CaP) mineral shell and Fe_3O_4 nanoparticles were doped simultaneously into the shell to endow bacteria with magnetic functionality (designed as B–MCaP). After adsorption of sodium monododecyl phosphate (MDP) on the mineral shell, the hydrophilic B–MCaP became interfacially active (B–MCaPS) facilitating the stabilization of Pickering emulsions, analogous to other surface-active particles as reported by our group and others.[6] Importantly, by immobilizing bacteria individually and optimizing the hydrophobic/hydrophilic balance of the mineral shell, inner diffusional limitations in the supports were clearly

[*] Z. Chen, H. Ji, C. Zhao, E. Ju, Prof. Dr. J. Ren, Prof. Dr. X. Qu
Laboratory of Chemical Biology and State Key Laboratory of Rare Earth Resource Utilization
Graduate School of the Chinese Academy of Sciences
Changchun, Institute of Applied Chemistry
Chinese Academy of Sciences, Changchun, Jilin 130022 (China)
E-mail: jren@ciac.ac.cn
xqu@ciac.ac.cn

[**] This work was supported by National Basic Research Program of China (Grants 2012CB720602 and 2011CB936004) and the National Natural Science Foundation of China (Grants 21210002, 91213302, 21431007, 21202158, and 91413111).

Supporting information for this article is available on the WWW under http://dx.doi.org/10.1002/anie.201412049.

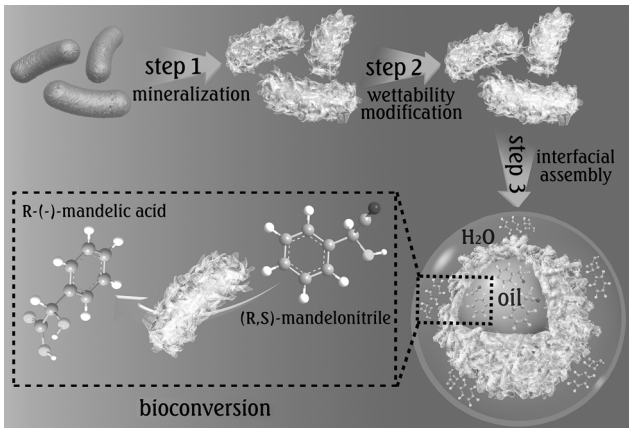

Scheme 1. The preparation of robust Pickering interfacial biocatalysts based on the individual bacterium encapsulation technique and their application in phase-transfer stereoselective bioconversion. In step 1, a calcium phosphate mineral shell doped with Fe_3O_4 nanoparticles was deposited onto the bacterial surface. In step 2, the wettability of the mineral shell was tailored by adsorption of MDP. In step 3, individually encapsulated bacteria were assembled at Pickering interfaces for hydrolyzing hydrophobic (*R,S*)-mandelonitrile in the oil phase into hydrophilic *R*-(−)-mandelic acid.

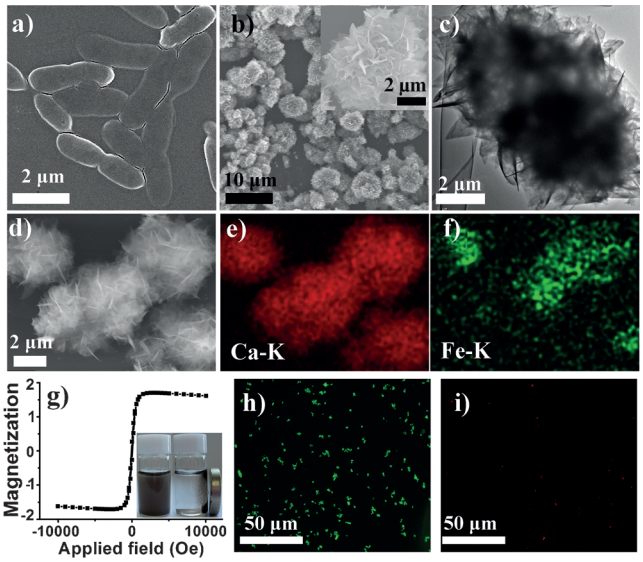

Figure 1. SEM images of a) bare *A. faecalis* ATCC 8750 bacteria and b) the individually mineralized bacteria (B–MCaP). Inset in (b): high-resolution SEM image. c) TEM image of B–MCaP. d–f) SEM image of B–MCaP for elemental mapping analysis of the system. Scale bar in (d–f) = 2 μm. g) Magnetization (emu g^{-1}) curve of B–MCaP. Inset in (g): photograph of B–MCaP in water (left) and their response to the external magnetic field (right). B–MCaP cells were treated with h) fluorescein diacetate (FDA) and i) propidium iodide (PI) for live/dead staining (live: green, dead: faint red).

decreased. Moreover, the direct location of individually encased bacteria at Pickering interfaces greatly enhanced the water–biocatalyst–oil interfacial areas, which diminished external diffusional limitations. With both external and internal diffusional limitations minimized, the catalytic performance was significantly improved. Most interestingly, the magnetic mineral shell not only facilitated the in situ product separation and recycling of the bacteria, but also effectively protected the whole cell from long-term organic-solvent stress. These benefits were demonstrated by the efficient reusability of the biocatalysts up to 30 cycles while retaining the high stereoselective catalytic activities, cell viabilities, and proliferative abilities.

To prepare individually encapsulated *A. faecalis* ATCC 8750 cells, one cycle of poly(allylamine hydrochloride) and poly(styrene sulfonate) were assembled on the surfaces of the bacteria to induce heterogeneous CaP nucleation (see Figure S1 in the Supporting Information).[7] Simultaneously, Fe_3O_4 nanoparticles were doped into the mineral shell (Figure S2). Scanning electron microscopy images (SEM; Figure 1 a, b), high-resolution SEM (inset in Figure 1 b), transmission electron microscopy (TEM; Figure 1 c) and optical microscopy images (Figure S3) clearly showed that the surfaces of the mineralized bacteria were covered by numerous flake-like nanocrystals which stacked to form porous structures with a thickness of about 1.5 μm. The presence of calcium and Fe_3O_4 in the mineral shell was demonstrated by element mapping using energy dispersive X-ray spectroscopy (Figure 1 d–f). Figure 1 g shows the superparamagnetic behavior of the B–MCaP hybrids by plotting the magnetization of the sample against the applied field. Using the reagents fluorescein diacetate (FDA) and propidium iodide (PI; Figure 1 h, i), the viability of the encapsulated cells was measured to be approximately 95% after mineralization, indicating that the encapsulation processes were compatible with the bacteria. As inferred from the permeability of FDA, the porous shell would be permeable to other enzymatic substrates,[5] an important prerequisite for biocatalysis.

Next, we tested the interfacial activity of the individually mineralized bacteria with toluene/water biphasic systems. Unfortunately, the B–MCaP-stabilized emulsion phases separated completely after shaking (Figure 2 a) because the B–MCaP was too hydrophilic to be surface active.[6] Intriguingly, further modifying the mineral-shell surfaces with MDP (Figure S4) through phosphate–calcium interactions was effective to render B–MCaP interfacially active. The resultant B–MCaPS were denoted B–MCaPS(*n*), where *n* represents the initial MDP concentration used. The stability of the Pickering emulsions obtained by employing the B–MCaPS systems was greatly enhanced and even phase inversion was observed (Figure 2). Up to 0.9 mg mL^{-1} MDP, emulsions were of the oil-in-water (o/w) type, whereas at 1.5 and 3 mg mL^{-1} MDP, water-in-oil (w/o) emulsions were formed. The appearance and the type of the emulsion were further confirmed by fluorescence microscopy (Figure 2 b–f) and conductivity variation (Figure S5). These phenomena could be attributed to the partial hydrophobization of the mineral shell by adsorption of MDP with the phosphate groups adsorbed on the CaP shell and the hydrocarbon chains protruding into the water, as indicated by the zeta-potential measurements (Figure S6), the adsorption isotherm (Figure S7), and the water contact-angle variations (θ; Figure S8). It is clear that tuning the amount of MDP adsorbed on the mineral shell could change the hydrophobicity of the B–MCaP to different

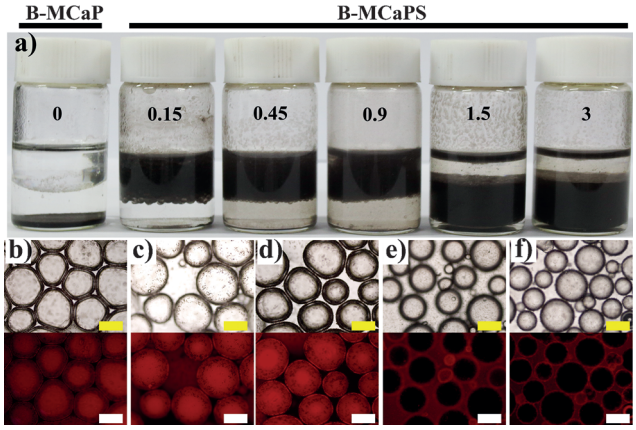

Figure 2. Interfacial activity of the individually encapsulated bacteria. a) The appearance after 24 h of toluene/water Pickering emulsions (1:1 by volume) stabilized by B–MCaP and B–MCaPS; the numbers represent the initial concentration ($mg\,mL^{-1}$) of monododecyl phosphate used to tailor the wettability of the mineral shell. b–f) Fluorescence microscopy images corresponding to the B–MCaPS(*n*)-stabilized Pickering emulsions shown in (a). b) $n = 0.15\ mg\,mL^{-1}$; c) $n = 0.45\ mg\,mL^{-1}$; d) $n = 0.9\ mg\,mL^{-1}$; e) $n = 1.5\ mg\,mL^{-1}$; f) $n = 3\ mg\,mL^{-1}$. Nile red was dissolved in the toluene phase to confirm the emulsion type. Scale bar in (b–f) = 200 μm.

degrees. Thus, different types of Pickering emulsions were formed.

Before utilizing B–MCaPS as a Pickering interfacial biocatalyst, the distribution of B–MCaPS at Pickering interfaces was clearly demonstrated by 2D/3D confocal fluorescence microscopy (Figure 3a), *Z*-optical axis confocal imaging (Figure S9, S10), and optical microscopy (Figure S11). The activity of these B–MCaPS as Pickering interfacial biocatalysts was then studied. The specific activity (dry cell weight (DCW), $\mu mol\,min^{-1}\,mg^{-1}$) of the individually encapsulated bacteria was plotted against the mandelonitrile concentration (Figure 3b). The specific activity of B–MCaPS(0.45) increased faster than that of B–MCaPS(0.15) as the concentration of mandelonitrile increased. Interestingly, as for B–MCaPS(0.9), the specific activity gradually increased until the mandelonitrile concentration reached 200 mM. For concentrations greater than 200 mM, decreased activity was observed. More interestingly, a similar trend was observed for B–MCaPS(1.5) and B–MCaPS(3), however the activity began to decrease at a much lower mandelonitrile concentration. These results indicated that the hydrophilic/hydrophobic nature of the artificial shell played a key role in determining the catalytic activity. As previously suggested for immobilized microbes, reducing the immobilization support size was an obvious way to overcome internal diffusional limitations and rational adjustment of the hydrophilic/hydrophobic balance of the supports would favor inner diffusion and the partitioning of hydrophobic substrates.[1c,8] In particular, the optimum composition of the support materials has also been shown to be strongly dependent on the existence and the degree of the substrate inhibitory effect.[1c] Thus, we could infer that for the least hydrophobic B–MCaPS, the increased specific activity was due to the facilitated diffusion and partitioning of the hydrophobic mandelonitrile substrate into the microenvironment around the bacteria. Even though B–MCaPS with higher θ values were more accessible to substrates, the decreased specific activity was mainly caused by the low substrate concentration tolerance of nitrilase (typically < 40 mM[9]). Furthermore, the kinetics of B–MCaPS(0.45) at Pickering interfaces followed Michaelis–Menten kinetics (Figure S12), indicating no substrate inhibition appeared in the tested concentration range. Therefore, by immobilizing bacteria individually and fine-tuning the hydrophilic/hydrophobic balance of the mineral shell, inner diffusional limitations could be effectively minimized while avoiding the high-substrate-concentration inhibitory effect.

Next, the bioconversion efficiency of B–MCaPS(0.45) at Pickering interfaces was tested (case 1). For comparison, control experiments with a collection of bacteria located in the droplet interior of SiO_2-particle-stabilized Pickering emulsions (case 2, Figure S13) and a collection of bacteria immobilized in calcium alginate beads (case 3, Figure S14) were conducted. In case 1 (Figure 3c) the conversion of the reaction reached 90–95% at equilibrium, whereas for case 2 a much longer time was required to reach equilibrium. Furthermore, only about 40% of conversion after 24 h was detected in case 3. After normalization of the data (Figure S15), the specific activity in case 1 was 3.88 and 18.41 times higher than that in cases 2 and 3, respectively. It appears that the low catalytic efficiency in case 3 can be

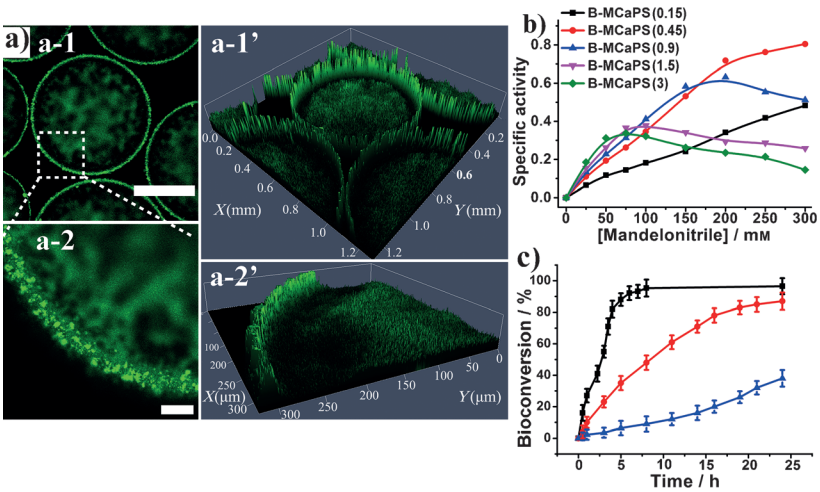

Figure 3. a) 2D (a-1; a-2) and 3D (a-1′; a-2′) confocal fluorescence microscopy of the distribution of fluorescein-labeled B–MCaPS at Pickering interfaces. In the high-resolution image (a-2), the B–MCaPS appear as green dots. Scale bars: a-1 = 200 μm; a-2 = 30 μm. b) The specific activity (DCW, $\mu mol\,min^{-1}\,mg^{-1}$) of B-MCaPS(*n*) at different substrate concentrations. c) The bioconversion of mandelonitrile by bacteria was investigated under different conditions, using B–MCaPS(0.45) as the Pickering interfacial biocatalyst (black line) and through control experiments where bacteria were dispersed in the interior of SiO_2-microparticle-stabilized Pickering emulsion droplets (red) and immobilized in alginate beads (blue).

attributed to the existence of external and internal diffusional limitations. Although the interfacial areas could be dramatically enlarged and mass transfer could be improved in case 2, the slower conversion was a result of the internal diffusional limitations within the droplets. In contrast, in case 1 the location of individually immobilized bacteria directly at Pickering interfaces greatly enhanced bioconversion performance. This enhancement was due to the physically facilitated transfer and partitioning of a substrate around the bacteria cell with both minimized internal and external diffusional resistances.

Another important aspect of using individually immobilized bacteria as Pickering interfacial biocatalysts was their magnetic properties. With a strong magnetic field ($B_r = 1.42$ T), complete phase separation was observed (Figure 4a). When the magnet was removed, emulsions could be formed again following homogenization. This effect was highly reversible and even after 30 cycles emulsions were still formed (Figure S16). This unique characteristic should facilitate the in situ recycling of the biocatalyst and enable the separation of products using a more bio-friendly method. Next, the hydrolysis of mandelonitrile samples was carried out using the recycled B–MCaP-(0.45) material as a Pickering interfacial biocatalyst. As shown in Figure 4b, high conversion efficiency above 80% was detected even after 30 cycles of use of the B–MCaP(0.45). Excitingly, the stereoselectivity remained almost constant during the successive reaction cycles (Table S1). Additionally, no division of the encapsulated bacterial cells was observed during the recycling reactions (Figure S17), indicating that the encapsulated bacteria are in a resting state. In contrast, low and decreased conversion was detected for bare microbes in control experiments. Specifically, negligible conversion was detected after 10 cycles for bare microbes.

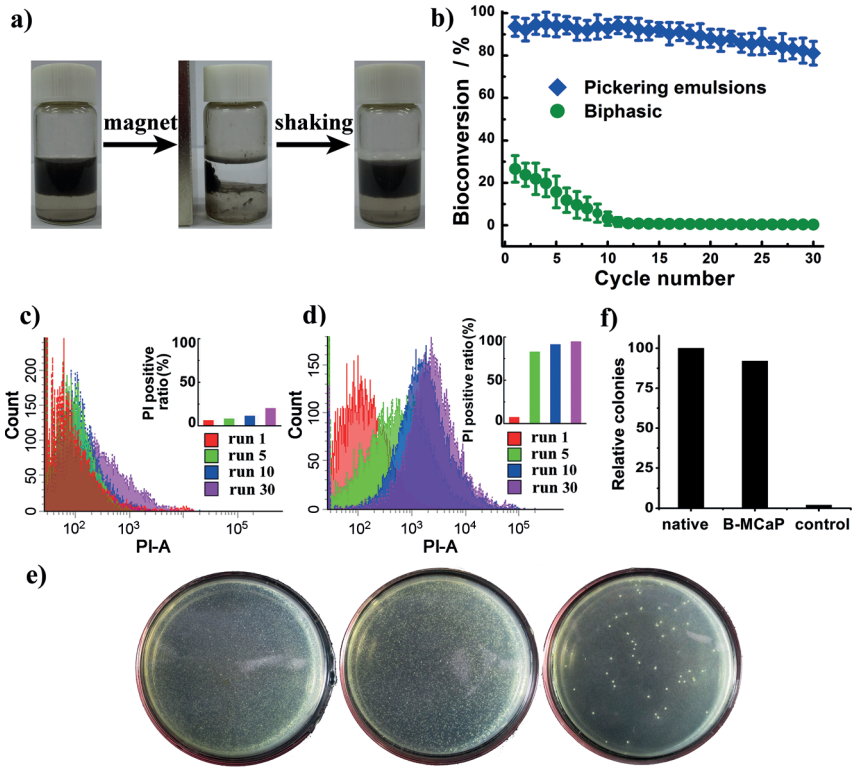

Figure 4. a) Magnetically controlled reversible disassembly and assembly of B–MCaPS(0.45) at Pickering interfaces. b) Recycling bioconversion efficiency of B–MCaPS(0.45) as a Pickering interfacial biocatalyst (blue) and bare bacteria in a biphasic system as a control experiment (green). c, d) Membrane integrity studies: flow-cytometry histograms of the fluorescence of PI in bacteria after different reaction cycles using c) B–MCaPS(0.45) and d) bare bacteria. The inset plots show the corresponding percentage of PI-positive cells obtained from the histograms. e) Colonies of bacteria grown under different conditions: the colonies of normal bacteria (left), colonies of the encapsulated bacteria after 30 reaction cycles (middle), and colonies of the bacteria from control experiments (right). f) Data corresponding to the colonies in (e).

It has been generally considered that cell membranes are the primary target of action by organic solvents[1c] and clearly it is the outer robust shell that protected the encapsulated cells herein from the organic-solvent stress, which was verified by flow cytometry (Figure 4c,d). It was evident that PI could barely penetrate the cell membrane of the encapsulated cells, while the membrane integrity of the bare bacteria decreased with increasing reaction cycles. Additionally, after degradation of the mineral shell by EDTA (ethylenediaminetetraacetic acid), the released bacteria proliferated like the normal cells (Figure 4e,f). These results confirmed that the mineral shell effectively protected bacteria from long-term organic-solvent stress through stabilization of cellular membranes and improved the operational stability of the whole-cell Pickering interfacial biocatalysts.

In addition to locating at toluene–water Pickering interfaces, we found that B–MCaPS was also able to stabilize emulsions using other organic solvents (Figure S18). Moreover, the individual-cell encapsulation technique has been well-established and has been shown to be a simple but widely applicable method to protect a series of cells.[5] Taken together, all these aspects implied that we have developed a powerful and versatile method for whole-cell-based long-term biphasic biocatalysis with minimized diffusional resistances.

In summary, whole-cell-based long-term and resistance-minimized biphasic biocatalysis was successfully realized by utilizing individually encapsulated *A. faecalis* ATCC 8750 cells as robust Pickering interfacial biocatalysts. By immobilizing bacteria individually and optimizing the hydrophobic/hydrophilic property of the mineral shell, individually encapsulated bacteria became interfacially active and localized at Pickering interfaces, which significantly minimized internal and external diffusional resistances and enhanced biocatalytic performances. Moreover, the incorporation of Fe_3O_4 into the shell endowed Pickering emulsions with magnetic properties,

which simplified in situ product separation and biocatalyst recycling. Most importantly, the robust mineral shell effectively protected the whole cell from long-term organic-solvent stress, as proven by the effective recycling ability of the biocatalysts up to 30 cycles while retaining high stereoselective catalytic activities, cell viabilities, and proliferative abilities. Overall, it is reasonable to expect that this powerful method can be further developed for application in biphasic whole-cell biocatalysis.

Keywords: biocatalysis · cell encapsulation · interfaces · nanostructures · phase transfer

How to cite: *Angew. Chem. Int. Ed.* **2015**, *54*, 4904–4908
Angew. Chem. **2015**, *127*, 4986–4990

[1] a) A. M. Klibanov, *Science* **1983**, *219*, 722; b) A. Schmid, J. S. Dordick, B. Hauer, A. Kiener, M. Wubbolts, B. Witholt, *Nature* **2001**, *409*, 258; c) R. León, P. Fernandes, H. M. Pinheiro, J. M. S. Cabral, *Enzyme Microb. Technol.* **1998**, *23*, 483; d) H. Pfründer, M. Amidjojo, U. Kragl, D. Weuster-Botz, *Angew. Chem. Int. Ed.* **2004**, *43*, 4529; *Angew. Chem.* **2004**, *116*, 4629.

[2] a) S. Crossley, J. Faria, M. Shen, D. E. Resasco, *Science* **2010**, *327*, 68; b) P. A. Zapata, J. Faria, M. P. Ruiz, R. E. Jentoft, D. E. Resasco, *J. Am. Chem. Soc.* **2012**, *134*, 8570; c) W. J. Zhou, L. Fang, Z. Fan, B. Albela, L. Bonneviot, F. De Campo, M. Pera Titus, J. M. Clacens, *J. Am. Chem. Soc.* **2014**, *136*, 4869; d) H. Yang, T. Zhou, W. Zhang, *Angew. Chem. Int. Ed.* **2013**, *52*, 7455; *Angew. Chem.* **2013**, *125*, 7603; e) Z. Wang, M. C. M. van Oers, F. P. J. T. Rutjes, J. C. M. van Hest, *Angew. Chem. Int. Ed.* **2012**, *51*, 10746; *Angew. Chem.* **2012**, *124*, 10904; f) J. Liu, G. Lan, J. Peng, Y. Li, C. Li, Q. Yang, *Chem. Commun.* **2013**, *49*, 9558.

[3] B. P. Binks, T. S. Horozov in *Colloidal Particles at Liquid Interfaces* (Eds.: B. P. Binks, T. S. Horozov), Cambridge University Press, Cambridge, **2006**, pp. 1–51.

[4] a) X. Shen, J. Svensson Bonde, T. Kamra, L. Bülow, J. C. Leo, D. Linke, L. Ye, *Angew. Chem. Int. Ed.* **2014**, *53*, 10687; *Angew. Chem.* **2014**, *126*, 10863; b) P. Wongkongkatep, K. Manopwisedjaroen, P. Tiposoth, S. Archakunakorn, T. Pongtharangkul, M. Suphantharika, K. Honda, I. Hamachi, J. Wongkongkatep, *Langmuir* **2012**, *28*, 5729.

[5] a) B. Wang, P. Liu, W. Jiang, H. Pan, X. Xu, R. Tang, *Angew. Chem. Int. Ed.* **2008**, *47*, 3560; *Angew. Chem.* **2008**, *120*, 3616; b) G. Wang, R. Y. Cao, R. Chen, L. Mo, J. F. Han, X. Wang, X. Xu, T. Jiang, Y. Q. Deng, K. Lyu, S. Y. Zhu, E. D. Qin, R. Tang, C. F. Qin, *Proc. Natl. Acad. Sci. USA* **2013**, *110*, 7619; c) J. Borovička, W. J. Metheringham, L. A. Madden, C. D. Walton, S. D. Stoyanov, V. N. Paunov, *J. Am. Chem. Soc.* **2013**, *135*, 5282; d) E. H. Ko, Y. Yoon, J. H. Park, S. H. Yang, D. Hong, K. B. Lee, H. K. Shon, T. G. Lee, I. S. Choi, *Angew. Chem. Int. Ed.* **2013**, *52*, 12279; *Angew. Chem.* **2013**, *125*, 12505; e) J. H. Park, K. Kim, J. Lee, J. Y. Choi, D. Hong, S. H. Yang, F. Caruso, Y. Lee, I. S. Choi, *Angew. Chem. Int. Ed.* **2014**, *53*, 12420; *Angew. Chem.* **2014**, *126*, 12628; f) S. H. Yang, S. M. Kang, K. B. Lee, T. D. Chung, H. Lee, I. S. Choi, *J. Am. Chem. Soc.* **2011**, *133*, 2795; g) M. Martín, F. Carmona, R. Cuesta, D. Rondón, N. Gálvez, J. M. Domínguez-Vera, *Adv. Funct. Mater.* **2014**, *24*, 3489; h) R. F. Fakhrullin, Y. M. Lvov, *ACS Nano* **2012**, *6*, 4557; i) R. F. Fakhrullin, A. I. Zamaleeva, R. T. Minullina, S. A. Konnova, V. N. Paunov, *Chem. Soc. Rev.* **2012**, *41*, 4189; j) J. H. Park, S. H. Yang, J. Lee, E. H. Ko, D. Hong, I. S. Choi, *Adv. Mater.* **2014**, *26*, 2001; k) C. Huang, G. Yang, Q. Ha, J. Meng, S. Wang, *Adv. Mater.* **2015**, *27*, 310.

[6] a) Z. Chen, L. Zhou, W. Bing, Z. Zhang, Z. Li, J. Ren, X. Qu, *J. Am. Chem. Soc.* **2014**, *136*, 7498; b) I. Kosif, M. Cui, T. P. Russell, T. Emrick, *Angew. Chem. Int. Ed.* **2013**, *52*, 6620; *Angew. Chem.* **2013**, *125*, 6752; c) M. Li, R. L. Harbron, J. V. Weaver, B. P. Binks, S. Mann, *Nat. Chem.* **2013**, *5*, 529; d) J. Jiang, Y. Zhu, Z. Cui, B. P. Binks, *Angew. Chem. Int. Ed.* **2013**, *52*, 12373; *Angew. Chem.* **2013**, *125*, 12599; e) H. Duan, D. Wang, N. S. Sobal, M. Giersig, D. G. Kurth, H. Möhwald, *Nano Lett.* **2005**, *5*, 949; f) C. Wu, S. Bai, M. B. Ansorge-Schumacher, D. Wang, *Adv. Mater.* **2011**, *23*, 5694; g) S. Wiese, A. C. Spiess, W. Richtering, *Angew. Chem. Int. Ed.* **2013**, *52*, 576; *Angew. Chem.* **2013**, *125*, 604; h) S. Melle, M. Lask, G. G. Fuller, *Langmuir* **2005**, *21*, 2158; i) Z. G. Cui, C. F. Cui, Y. Zhu, B. P. Binks, *Langmuir* **2012**, *28*, 314; j) X. Shen, L. Ye, *Macromolecules* **2011**, *44*, 5631; k) X. Yao, Y. Song, L. Jiang, *Adv. Mater.* **2011**, *23*, 719; l) W. Guo, C. Cheng, Y. Wu, Y. Jiang, J. Gao, D. Li, L. Jiang, *Adv. Mater.* **2013**, *25*, 6064; m) M. Hermes, P. S. Clegg, *Soft Matter* **2013**, *9*, 7568; n) J. W. Tavacoli, J. H. J. Thijssen, A. B. Schofield, P. S. Clegg, *Adv. Funct. Mater.* **2011**, *21*, 2020.

[7] Z. Chen, Z. Li, Y. Lin, M. Yin, J. Ren, X. Qu, *Biomaterials* **2013**, *34*, 1364.

[8] M. T. Reetz, A. Zonta, J. Simpelkamp, *Angew. Chem. Int. Ed. Engl.* **1995**, *34*, 301; *Angew. Chem.* **1995**, *107*, 373.

[9] a) K. Yamamoto, I. Fujimatsu, K. I. Komatsu, *J. Ferment. Bioeng.* **1992**, *73*, 425; b) Z. J. Zhang, J. H. Xu, Y. C. He, L. M. Ouyang, Y. Y. Liu, T. Imanaka, *Process Biochem.* **2010**, *45*, 887.

Received: December 16, 2014
Revised: January 18, 2015
Published online: February 23, 2015

